

# Investigation of Trail Formation with the Active Walker Model

Anuj Girdhar and James Antonaglia

May 6, 2013

## Abstract

When traveling to a destination, both humans and animals generally attempt to optimize the chosen path by minimizing either the distance traveled or the time spent traveling. However, these "optimal" paths may not necessarily be the most comfortable, depending on the terrain and any obstacles encountered on these paths. Deviations from time-optimized paths lead the walkers to alternate routes with comfort levels greater than the optimal ones, and the walkers' subsequent interactions with their environment create new paths or can reinforce old ones. We study a simple model of active walkers that interact with a comfort field on their way to a destination. We show that sufficiently strong interactions between the walkers and their environment cause the emergence of trail networks, and we analyze both the efficiency of these trails as well as the degree to which these trails are utilized by active walkers.

## 1 Introduction and Motivation

Given an open walking region, a person or animal traveling from one point in the region to another generally optimizes some aspect of the pathway she will walk. A direct line path from origin to destination minimizes the distance traveled, but may not minimize the time, taking inhomogeneous and rough terrain into consideration. However, a walker traipsing on difficult—but malleable—terrain such as snow or vegetation leaves lasting footprints. The next walker to traverse the landscape will no doubt take the same path because of the ease of travel these footprints provide, reinforcing the freshly made trail. Over time, lasting trail formations develop, creating large networks which gradually change over time.

This effect is most prominently seen in ant colonies [1], who, in the search for food, lay down chemical signals to mark their trails. Other ants that fall upon these trails move along them and

reinforce the strength of any signals encountered. Trails that are long and winding, and thus inefficient, are traveled less often than trails that route to a food source succinctly and efficiently. As a result, these winding trails die away and leave a strong path visible to any ant in the colony to a food source.

In this study, we explore generic walkers moving between destinations on a map while interacting with the terrain. We will show that the trails formed in this way organize into structures that look like road networks, and we contrast this with a model in which no interactions with the environment are considered. A model with no interactions produces a complete graph between all possible destinations; each pathway is a geodesic which minimizes distance. However, this configuration does not minimize the total area covered by all trails, which is of practical importance for urban planners, foresters, and architects, to whom total area is proportional to cost. By allowing interactions with the landscape, walkers can produce trails with small total path distance at the expense of longer paths between destinations.

In general, the interactions of walkers with their terrain involve many tuneable parameters, specifically the rate of regeneration of terrain, the intensity of walkers' footsteps, and the visibility ("line of sight" distance). Our goal is to study the emergence of trail formations as a function of these various parameters.



Figure 1: *Park space of the University of Brasilia*—Trails are made in the grass by the footprints of walkers, and trails that have begun are reinforced by walkers who decide to maximize comfort over minimizing time of travel. The trail networks evident in the lawn remain because the rate of regeneration of the rough terrain is much lower than the rate of traversal by walkers [3].

## 2 Model and Theory

The active walker model consists of  $N$  walkers in an  $L \times L$  box with hard (reflective) boundaries. There are  $d$  potential destinations that act as either sources or sinks for the walkers. Walkers are uniformly and randomly assigned a source and a sink (such that the sink and source are not the same position). When a walker reaches her destination, she stops, exits the field, and a new walker begins a new, random source-sink walk (i.e. the number of walkers on the field at any given time is always  $N$ ).

The equation of motion of the  $i$ th walker is [2]:

$$\vec{f}(\vec{r}, t) = \frac{1}{\tau}(v_0\vec{e}(\vec{r}) - \vec{v}(t)) - \vec{\nabla}V(\vec{r}) + \vec{\xi}(t) \quad (1)$$

where  $V$  is the gravitational potential that describes the landscape of the field (set to 0 in the simplest cases),  $\vec{e}$  is a unit vector in the walker's desired direction,  $\vec{\xi}$  is uncorrelated Gaussian noise with amplitude  $\sigma$ , and  $\tau$  is the walker's relaxation time [2]. The direction  $\vec{e}$  is determined by the direction to the walker's destination and the presence of paths around the walker. To describe the presence of a path, we define a scalar field  $G(\vec{r})$ ; large values of  $G$  are interpreted as "comfortable" paths at the position  $\vec{r}$ . The walker, upon each step, looks for paths around it, such that a portion of the field with area  $d^2r$  that has comfort  $G(\vec{r})$  attracts the walker such that the total force is:

$$\vec{f}_{i, trail} = \int d^2r \frac{(\vec{r} - \vec{r}_i)}{|\vec{r} - \vec{r}_i|} \exp(-|\vec{r} - \vec{r}_i|/\sigma) G(\vec{r}) / (2\pi\sigma^2) \quad (2)$$

This formulation produces an attractive force towards trails only within a radius  $\sigma$  of the walker, characterizing the visibility. The force  $\vec{f}_{i, trail}$  is averaged with the force towards the destination  $\vec{f}_{i, dest}$  defined as:

$$\vec{f}_{i, dest} = \frac{\vec{r}_{i, dest} - \vec{r}_i}{|\vec{r}_{i, dest} - \vec{r}_i|} \quad (3)$$

$$\vec{e} = \frac{\vec{f}_{i, trail} + \vec{f}_{i, dest}}{|\vec{f}_{i, trail} + \vec{f}_{i, dest}|} \quad (4)$$

The field  $G(\vec{r})$  is dynamic in time; as walkers trample the terrain,  $G(\vec{r}, t)$  increases at the position of the walkers' footsteps, but  $G(\vec{r}, t)$  decreases in time as the terrain's roughness regenerates [2]. The regeneration rate simulates vegetation reclaiming trampled paths or snow falling to fill in footsteps. We model the dynamics of  $G(\vec{r}, t)$  as:

$$\frac{\partial G(\vec{r}, t)}{\partial t} = -\frac{G(\vec{r}, t)}{T(\vec{r})} + I(\vec{r}) \left( 1 - \frac{G(\vec{r}, t)}{G_{max}(\vec{r})} \right) \sum_i^N \delta(\vec{r} - \vec{r}_i) \quad (5)$$

The function  $T(\vec{r})$  sets the time-scale for the regeneration of terrain. The field  $I(\vec{r})$  describes the intensity of walkers' footsteps. The term  $G_{max}(\vec{r})$  defines the saturation value of the comfort field  $G(\vec{r}, t)$  to prevent it from growing without bound [2]. This also produces the effect of trail deterioration by over-use: if  $G > G_{max}$ , then the footsteps have a detrimental effect on the pathway, but this effect is not seen in practice.

Helbing et. al in [2] characterize the trail networks they generate by measuring the qualitative paths that form. We define a systematic method to quantitatively characterize our trail networks by defining two parameters. The first is  $\epsilon$ , the efficiency of the trail network. We would like to define  $\epsilon$  to be small for trails that are spatially spread out and large for trails that are concise and well-defined. The second is  $c$ , the "civility" of a walk. This parameter sums the values of  $G(\vec{r}, t)$  along the path of a particular walker and averages over the total number of footsteps over that path.

### 3 Methods and Implementation

Using time steps of  $\Delta$ , the walkers progress in time according to a simple Verlet velocity algorithm borrowed from molecular dynamics simulations [4] (setting mass to 1):

$$\vec{r}(t + \Delta) = 2\vec{r}(t) - \vec{r}(t - \Delta) + \Delta^2 \vec{f}(t) \quad (6)$$

$$\vec{v}(t + \Delta) = \frac{1}{\Delta} (\vec{r}(t + \Delta) - \vec{r}(t)) \quad (7)$$

Here,  $\vec{f}$  is calculated from Equation 1 from the positions of the trails, destinations, etc.

The comfort field  $G(\vec{r}, t)$  is discretized into small square cells of width  $L/n$ , with  $n$  the number of cells on a side, which is amenable to a matrix representation. The fields  $T$ ,  $I$ , and  $G_{max}$  will also be discretized in the same way. The time evolution of  $G_{i,j}$  is simply:

$$G_{i,j}(t + \Delta) = \Delta \frac{\partial G_{i,j}(\vec{r}, t)}{\partial t} \quad (8)$$

The efficiency coefficient  $\epsilon$  will be defined as

$$\epsilon^{-1} = 1000 \sum_{\langle i,j \rangle \in \{i,j\}: G_{i,j} > I_{i,j}} \Theta(I_{i,j} - G_{i,j}) \quad (9)$$

Here,  $\Theta$  is the Heaviside step function. The notation  $\langle i, j \rangle$  denotes nearest neighbors. For every cell with  $G > I$ , which constitutes a segment of path, we count its nearest neighbors whose  $G < I$ . The factor of 1000 is chosen empirically to make the index  $\epsilon$  on the order of unity. This criterion was chosen because  $I$  represents the incremental increase in  $G$  from  $G = 0$  after one walker's footstep. This effectively measures the total length of the borders of the network. An intuitive interpretation would be the amount of curbside necessary to create roads along the network. Efficient networks are more compressed whereas inefficient networks are spread out and have large borders. We present the efficiency of the steady-state network structures, not the dynamic structures.

The second parameter we call the "civility," which should measure the average comfort that a walker experiences. For each walker, we sum up the comfort field  $G_{i,j}$  of every cell that the walker steps into. When the walker reaches its destination and leaves the field, this sum  $\sum_{\text{path}} G_{i,j}$  is divided by the number of steps taken.

$$c_k = \left( \sum_{\text{path of } k} G_{i,j} \right) / \left( \sum_{\text{path of } k} 1 \right). \quad (10)$$

Because there are many walkers taking many different paths, the value of  $c$  varies for each walker  $k$  and will be, in general, a function of time. As the  $G$  field evolves, we expect the average civility to increase to some steady-state value. A trail that has dense traffic will have a large equilibrium  $G$  value, and thus these walkers will have a high civility coefficient. Trails that do not channel lots of traffic will have low civility. Walkers that simply take the minimum distance route to their destinations will thus not collect together and form heavy-traffic areas, lowering their civility coefficient.

Using qualitative arguments of the form of  $G_{i,j}(t)$  and the parameters  $\epsilon$  and  $c$ , we will characterize:

- Vary the parameter  $\sigma$  and see its effect on the shape of the path network, i.e. the total path length, efficiency, average civility, connectivity of destinations, and qualitative features. The parameter  $\sigma$  controls the length scale of interactions (keeping  $v_0$  constant), so for large  $\sigma$  walkers' decisions are influenced by very many pathways, much like having a road-map available to read. For small  $\sigma$ , the model should produce results of walker movement when knowledge of existing trails is very limited, i.e., the walkers see what is around them and optimize comfort locally.
- Vary the parameters  $I$  and  $T$  to change the rate of change of the  $G$  field.  $I$  is essentially the coupling between the walkers and the field, and  $T$  controls the time scale of regeneration. Making both of these parameters large will create dense, long-lasting paths, whereas making these trails small will cause trails to disappear quickly.

- Alter the gravitational potential  $V(\vec{r})$ . When  $V = 0$ , the shortest distance path is given by the simple straight line geodesic. When the potential is nonzero, the straight-line paths will be deformed to new "geodesics." We will test whether the walkers, by interacting with each others' paths, can optimize a more complex landscape with features such as hills, valleys, and hard walls.

## 4 Results

A triangular configuration and asymmetric X-shaped configuration of destinations were tested for various values of  $\sigma$ , the line-of-sight parameter. We find that for small values of  $\sigma$ , the paths that form are tight and concise, whereas path networks for large  $\sigma$  tend towards the inefficient distance-minimizing pathways. The results for the efficiency parameter for these path networks are shown in Tables 1 and 2. Intensity maps of the comfort field  $G(\vec{r})$  at the end of the simulation are given in Figure 2.

$\sigma$	$\epsilon$
0.05	$4.80 \pm 0.15$
0.1	$3.87 \pm 0.07$
0.2	$3.42 \pm 0.01$
0.5	$3.23 \pm 0.02$

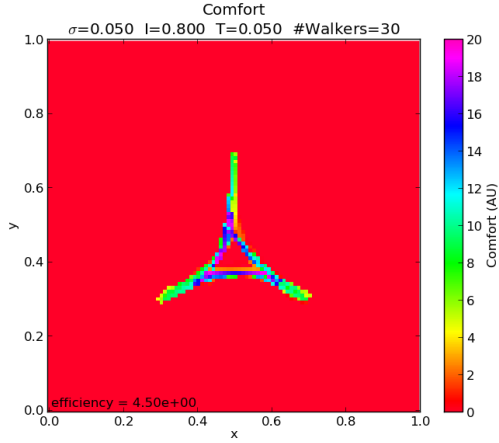
Table 1: Our measure of efficiency decreases as the line-of-sight parameter  $\sigma$  increases. As  $\sigma$  decreases, walkers couple tightly to paths around them and are less inclined to move directly to their destination. The error bars are calculated from variations in six repeated realizations of each  $\sigma$  value.

$\sigma$	$\epsilon$
0.05	$1.49 \pm 0.02$
0.1	$1.05 \pm 0.02$
0.2	$0.949 \pm 0.013$
0.5	$0.968 \pm 0.008$

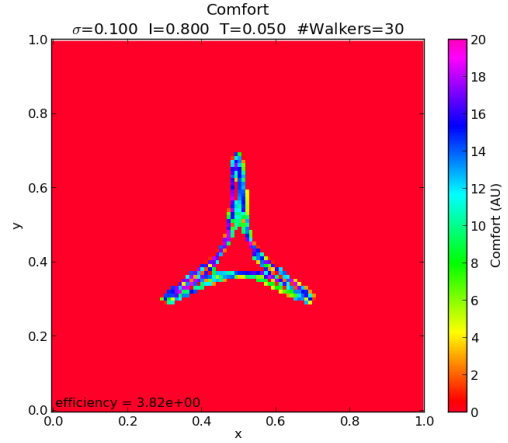
Table 2: The values of efficiency for the X-shaped path.

Next, we tested the effect of  $T$  and  $I$  on the structure of the trail network. We used a triangular array of destinations and an asymmetric X-shaped array of cities again. The results of the efficiency parameter are shown in Tables 3 and 4.

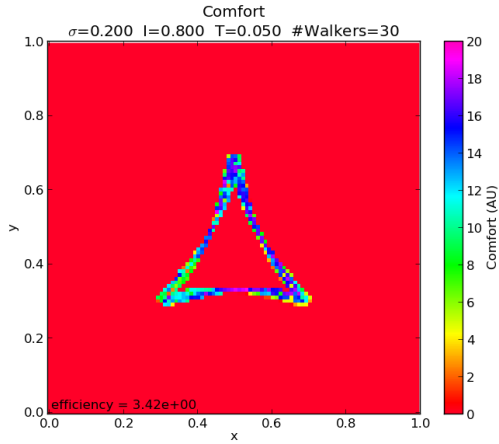
Lastly, we show the effect of static gravitational potential fields. Sufficiently complicated potentials will distort the straight-line paths connecting destinations into more intricate networks.



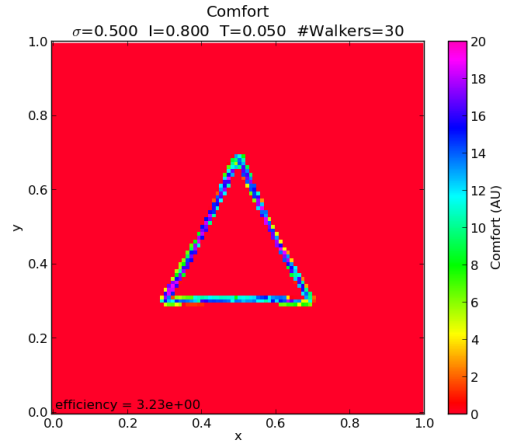
(a) Triangular configuration for  $\sigma = 0.05$ .



(b) Triangular configuration for  $\sigma = 0.1$ .

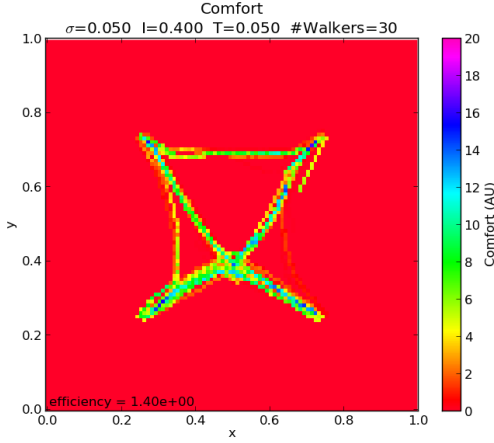


(c) Triangular configuration for  $\sigma = 0.2$ .

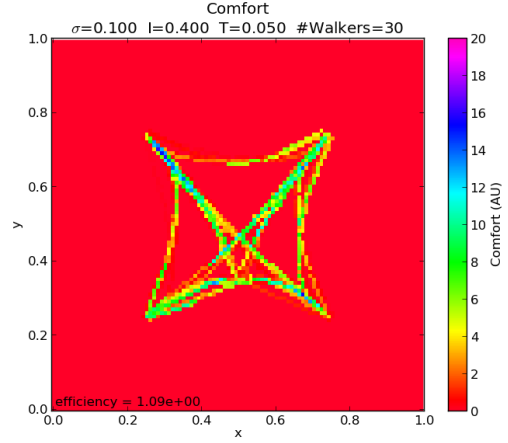


(d) Triangular configuration for  $\sigma = 0.5$ .

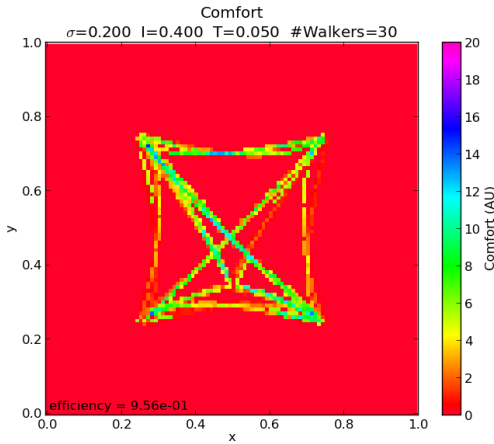
Figure 2: These plots show the steady-state networks for a triangular group of cities. The run time was 2000 time steps of  $\Delta = 0.0015$ ,  $G_{max} = 20$ ,  $I = 0.8$ ,  $T = 0.05$ ,  $v_0 = 20$ , and the number of walkers  $N = 30$ . The potential is flat, so when  $\sigma$  becomes large, the path network turns into straight lines between destinations.



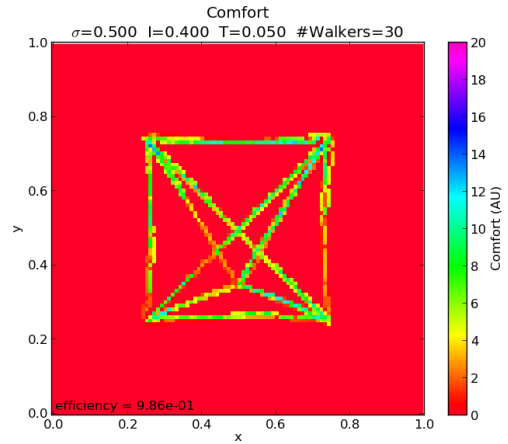
(a) X configuration for  $\sigma = 0.05$ .



(b) X configuration for  $\sigma = 0.1$ .



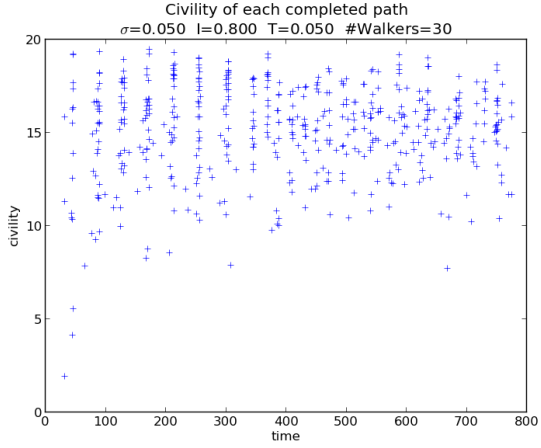
(c) X configuration for  $\sigma = 0.2$ .



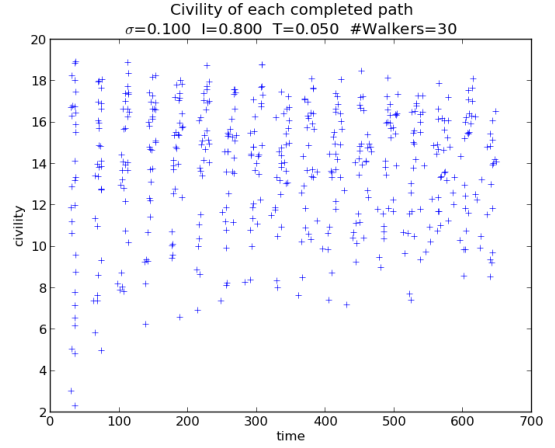
(d) X configuration for  $\sigma = 0.5$ .

Figure 3: These plots show the steady-state networks for the asymmetric X configuration. There are cities at the positions  $(0.25, 0.25)$ ,  $(0.25, 0.75)$ ,  $(0.75, 0.25)$ ,  $(0.75, 0.75)$ , and  $(0.5, 0.35)$  to break the symmetry. The run time was 2000 time steps of  $\Delta = 0.0015$ ,  $G_{max} = 20$ ,  $I = 0.4$ ,  $T = 0.05$ ,  $v_0 = 20$ , and the number of walkers  $N = 30$ . In this more complicated array of cities, the efficiency does not monotonically increase with decreasing  $\sigma$ .

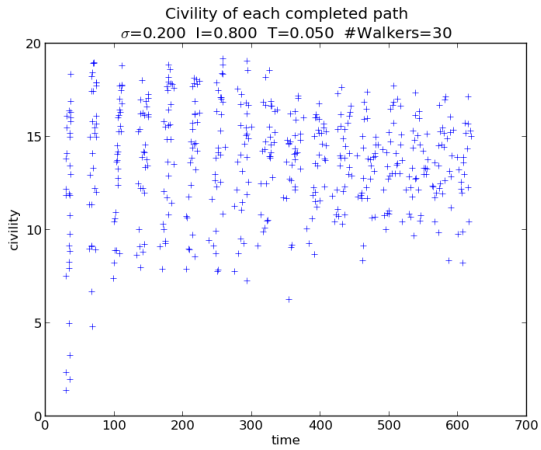




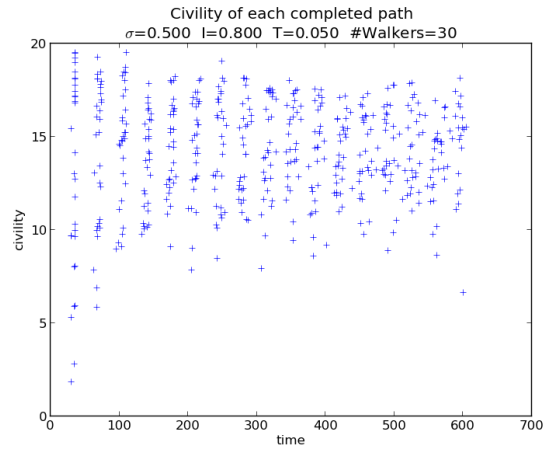
(a) Triangular configuration for  $\sigma = 0.05$ .



(b) Triangular configuration for  $\sigma = 0.1$ .

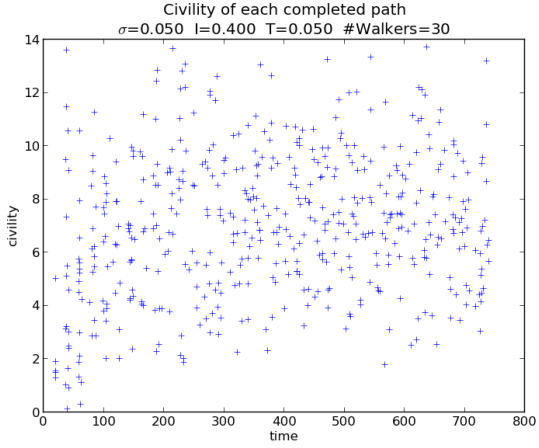


(c) Triangular configuration for  $\sigma = 0.2$ .

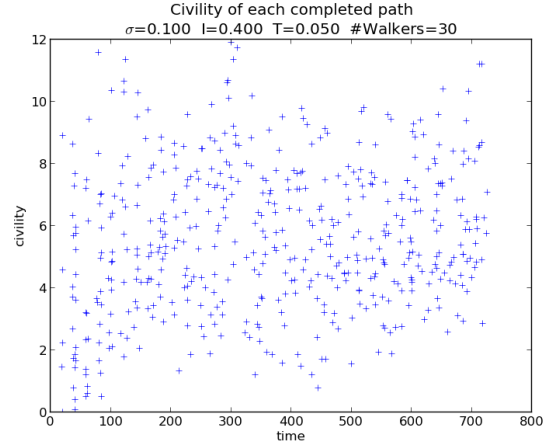


(d) Triangular configuration for  $\sigma = 0.5$ .

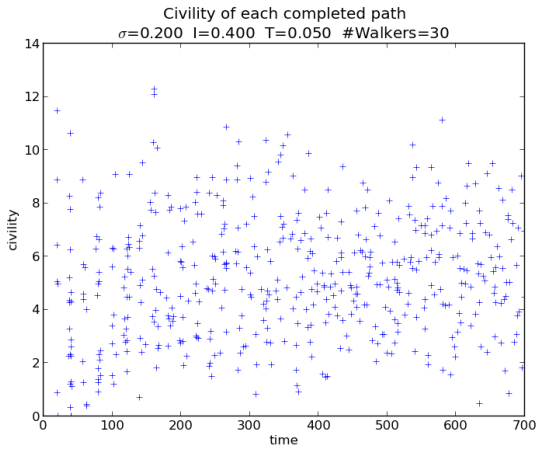
Figure 4: These plots show the dynamic civility coefficient for a triangular group of cities. The civility  $c(t)$  is the average value of  $G$  in a given walk that is completed at time  $t$ . As time progresses, these average  $G$  values should converge as the network settles to a steady state. Only the first few hundred time steps are shown, as the values saturate after about 1000 time steps.



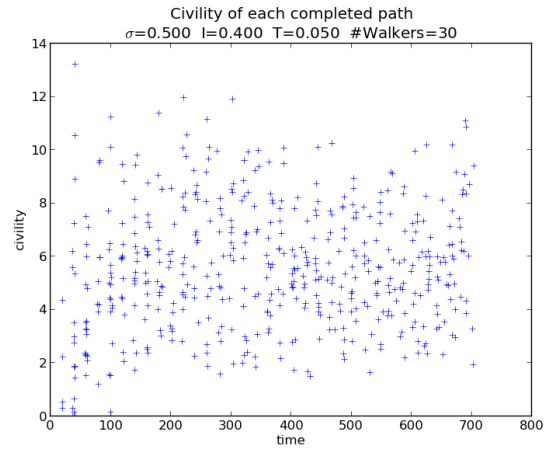
(a) X configuration for  $\sigma = 0.05$ .



(b) X configuration for  $\sigma = 0.1$ .

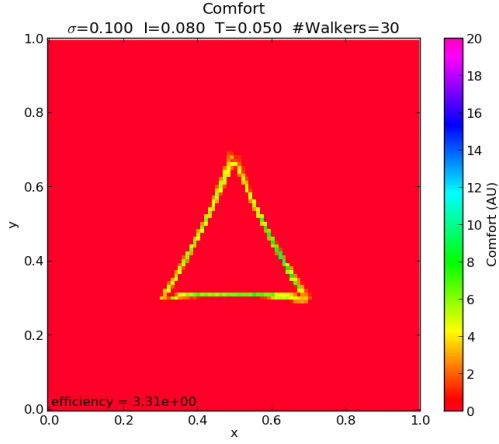


(c) X configuration for  $\sigma = 0.2$ .

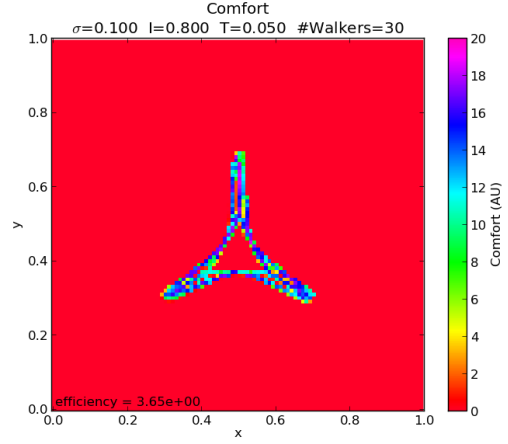


(d) X configuration for  $\sigma = 0.5$ .

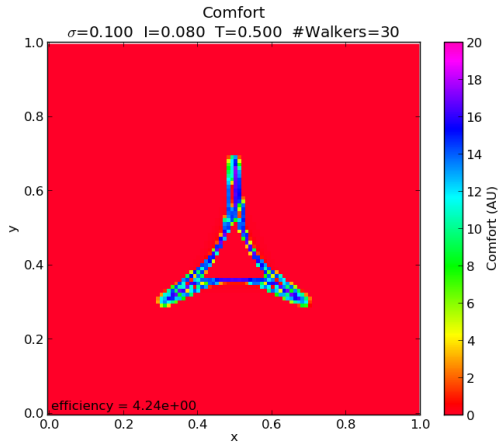
Figure 5: These plots show the dynamic civility coefficient for a square group of cities. The civility  $c(t)$  is the average value of  $G$  in a given walk that is completed at time  $t$ . As time progresses, these average  $G$  values should converge as the network settles to a steady state. Only the first few hundred time steps are shown, as the values saturate after about 1000 time steps.



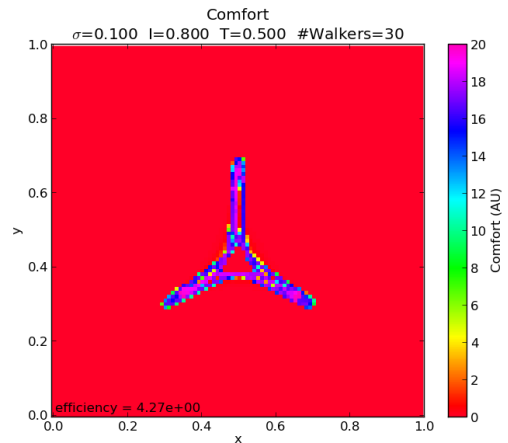
(a) Triangular configuration for  $T = 0.05$ ,  $I = 0.08$ .



(b) Triangular configuration for  $T = 0.05$ ,  $I = 0.8$ .

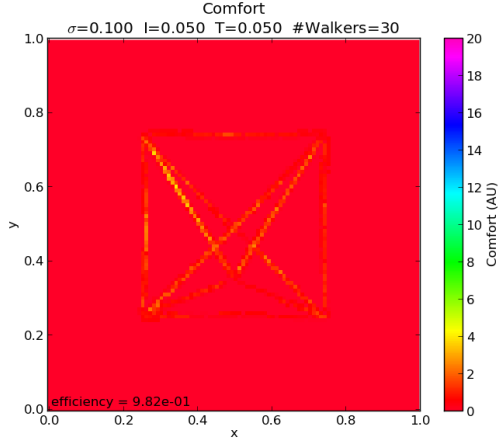


(c) Triangular configuration for  $T = 0.5$ ,  $I = 0.08$ .

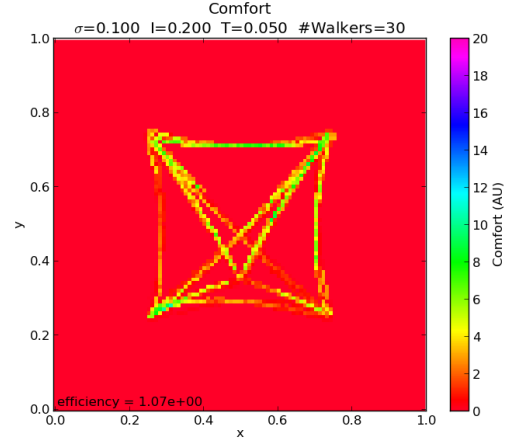


(d) Triangular configuration for  $T = 0.5$ ,  $I = 0.8$ .

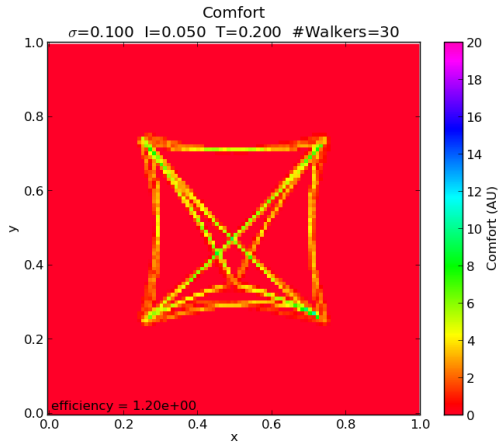
Figure 6: These plots show the steady-state networks for a triangular group of cities with varying  $T$  and  $I$ . The run time was 2000 time steps of  $\Delta = 0.0015$ ,  $G_{max} = 20$ ,  $\sigma = 0.1$ ,  $v_0 = 20$ , and the number of walkers  $N = 30$ . The potential here is again flat.



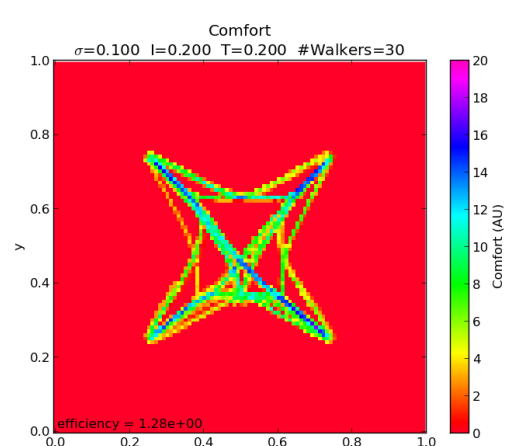
(a) Triangular configuration for  $T = 0.05$ ,  $I = 0.05$ .



(b) Triangular configuration for  $T = 0.05$ ,  $I = 0.2$ .

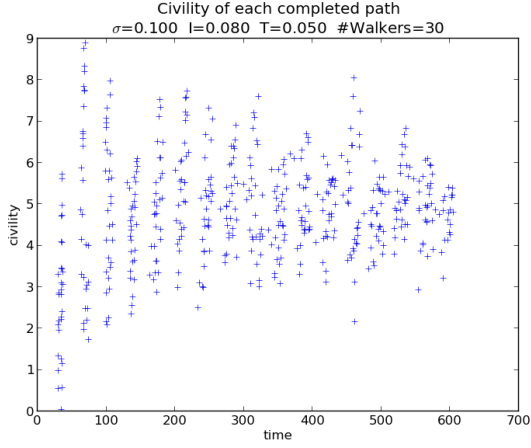


(c) Triangular configuration for  $T = 0.2$ ,  $I = 0.05$ .

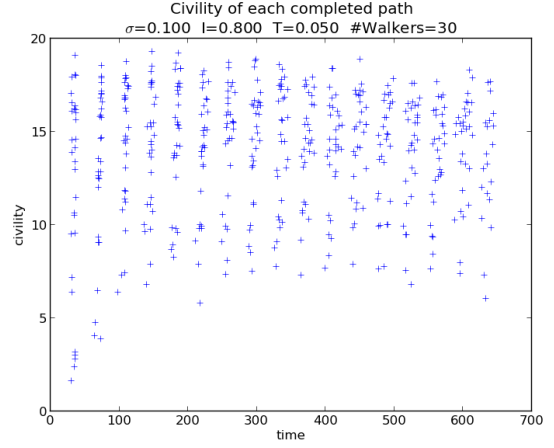


(d) Triangular configuration for  $T = 0.2$ ,  $I = 0.2$ .

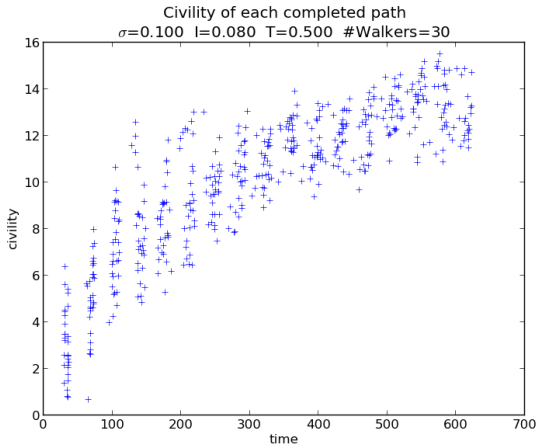
Figure 7: These plots show the steady-state networks for the X-shaped array of cities with varying  $T$  and  $I$ . The run time was 2000 time steps of  $\Delta = 0.0015$ ,  $G_{max} = 20$ ,  $\sigma = 0.1$ ,  $v_0 = 20$ , and the number of walkers  $N = 30$ . The potential here is again flat.



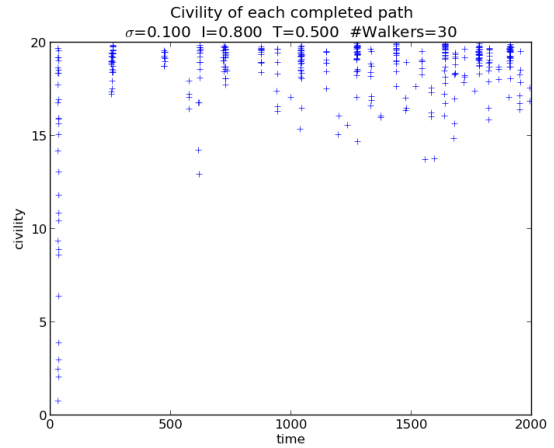
(a) Triangular configuration for  $T = 0.05$ ,  $I = 0.08$ .



(b) Triangular configuration for  $T = 0.05$ ,  $I = 0.8$ .

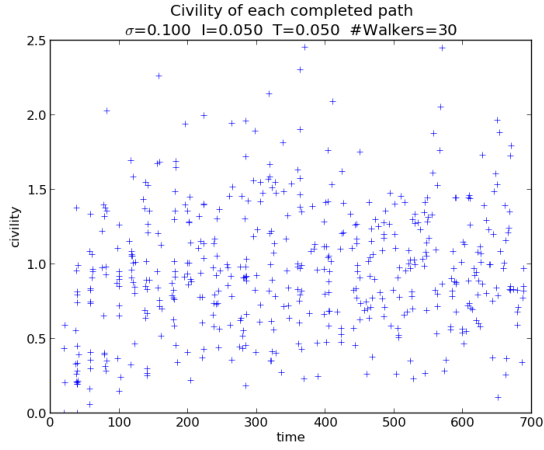


(c) Triangular configuration for  $T = 0.5$ ,  $I = 0.08$ .

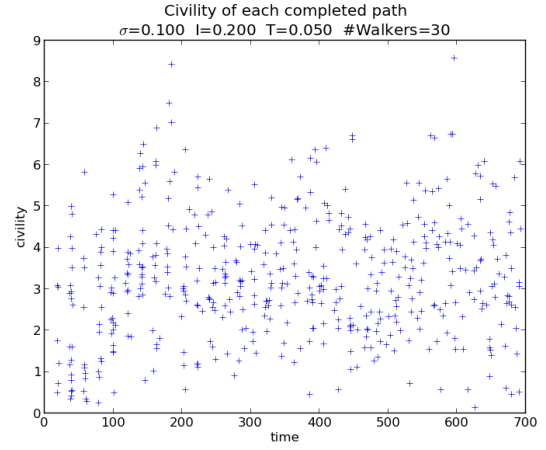


(d) Triangular configuration for  $T = 0.5$ ,  $I = 0.8$ .

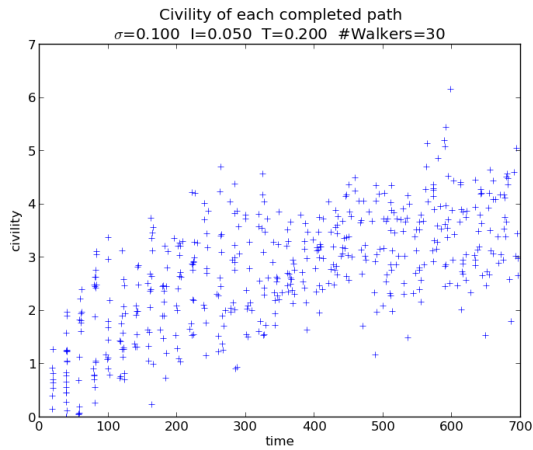
Figure 8: These plots show average  $G$  value, the civility  $c(t)$ , over paths that end at time  $t$  for a triangular group of cities with varying  $T$  and  $I$ . The run time was 2000 time steps of  $\Delta = 0.0015$ ,  $G_{max} = 20$ ,  $\sigma = 0.1$ ,  $v_0 = 20$ , and the number of walkers  $N = 30$ . The potential here is again flat. Only the first few hundred time steps are shown, as the values saturate after about 1000 time steps.



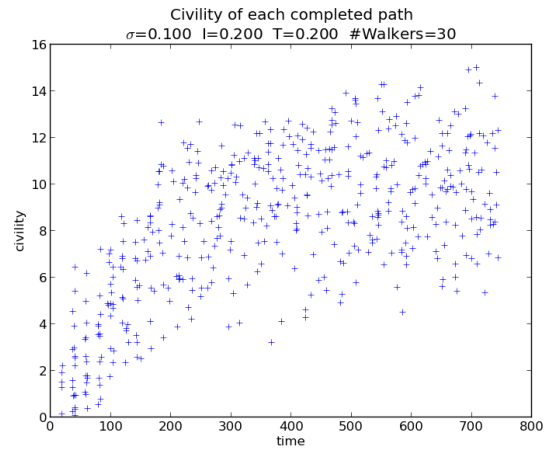
(a) X configuration for  $T = 0.05$ ,  $I = 0.05$ .



(b) X configuration for  $T = 0.05$ ,  $I = 0.2$ .



(c) X configuration for  $T = 0.2$ ,  $I = 0.05$ .



(d) X configuration for  $T = 0.2$ ,  $I = 0.2$ .

Figure 9: These plots show the dynamic civility coefficient for the asymmetric X configuration of cities. The civility  $c(t)$  is the average value of  $G$  in a given walk that is completed at time  $t$ . As time progresses, these average  $G$  values should converge as the network settles to a steady state. Only the first few hundred time steps are shown, as the values saturate after about 1000 time steps.

$T$	$I$	$\epsilon$
0.05	0.08	$3.27 \pm 0.01$
0.05	0.8	$3.69 \pm 0.07$
0.5	0.08	$4.19 \pm 0.02$
0.5	0.8	$4.44 \pm 0.06$

Table 3: This table shows the efficiency’s dependence on the time scale of comfort restoration  $T$  and the foostep intensity  $I$  for the triangular city configuration.

$T$	$I$	$\epsilon$
0.05	0.05	$0.991 \pm 0.006$
0.05	0.2	$1.055 \pm 0.008$
0.2	0.05	$1.181 \pm 0.007$
0.2	0.2	$1.298 \pm 0.015$

Table 4: The efficiency’s dependence on the time scale of comfort restoration  $T$  and the foostep intensity  $I$  for the X configuration.

Our goal was to see if this added complexity made it more difficult for the walkers to optimize the trail network.

The potentials we tested were a double-hill system of Gaussian-shaped bumps with potential functions

$$V_1(x, y) = 400 \exp\left(\frac{-(x - 0.1)^2 - (y - 0.3)^2}{0.08}\right) + 1000 \exp\left(\frac{-(x - 0.7)^2 - (y - 0.6)^2}{0.02}\right). \quad (11)$$

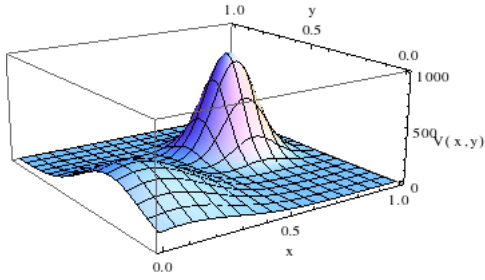
$$V_2(x, y) = 1000 \cos^2(2\pi y) \exp(-60(x - 0.5)^2) \quad (12)$$

$V_1$  is the potential of two steep hills, one at (0.1,0.3) and one at (0.7,0.6).  $V_2$  is a ravine system with a "mountain range" and two passages through it. Surface plots of these potentials are shown in Figure 10.

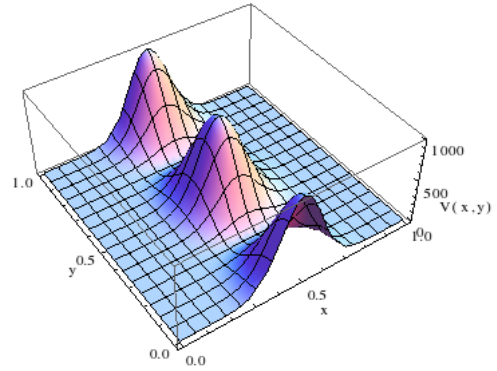
For each potential, we do a single run for each of two values of  $\sigma$ , to see qualitatively how the potentials affect the distribution of paths.

## 5 Discussion

All the tuneable parameters had to be chosen carefully such that the walkers actually finished their paths. In Figure 13, we show how walkers can be too attracted to the pathways and not enough to their destination in a phenomenon we have called pooling.



(a) Gaussian hill potential.



(b) Ravine or mountain range potential.

Figure 10: Potentials used to test how much the walkers could affect the complex geodesic paths.

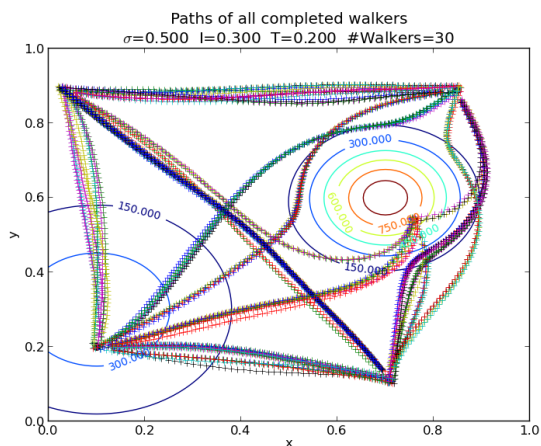
Tables 1–4 show that with decreasing  $\sigma$ , the path networks increase in efficiency. This effect is evident in Figure 2; as  $\sigma$  decreases, the paths pinch together and eliminate area between them. The average length of paths between destinations increase, but all together, this corresponds to a decrease in the total path length. This agrees with the results of [2], in which the experiment was performed on the triangular configuration, whose results we replicate. The X formation (Figure 3) is our own result, where the path-pinching effect is also seen. With the X formation, we implemented a destination that was nearby, but not directly on, a straight-line path between two other destinations. As the parameter  $\sigma$  decreased and coupling to the path became stronger, the off-center middle city became a way-point for walkers crossing from one corner to the other.

Figure 4 shows that the civility increases as time progresses, because the walkers adjust their paths to ones with increased comfort. The average civility saturates as the map equilibrates. The initial walkers enjoy no comfort whatsoever, so their civility (total comfort per step) is low. As the trails become more defined, each step experiences an increased comfort, increasing the civility as well.

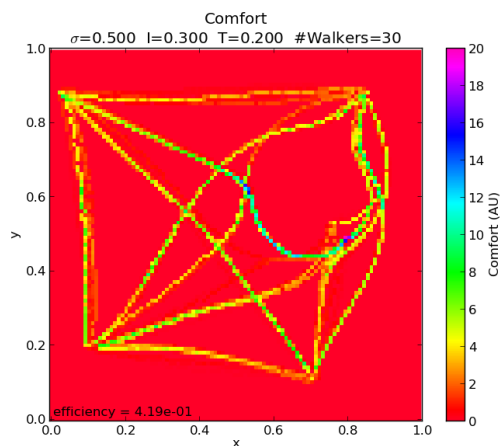
In general, as the intensity of stepping  $I$  increases, the civility should increase as well, seen in both figures 4 and 5. A large  $I$  should also increase the variance in civilities for a given trail formation, because the change in comfort after each step is larger. Additionally, a larger regeneration rate (smaller  $T$ ) should cause a larger variance and smaller average value of civility, as the path deteriorates more quickly, causing the total comfort of a path to decrease more quickly for the next walker. This is indeed seen in both figures.

The addition of gravitational potential hills alters the chosen paths to ones that avoid them. As seen in figures 11 and 12, walkers tend to walk around the hills even if a city is on top of one. The paths tend to go through areas between adjacent hills even if the straight line path goes over one of them. However, this behavior is expected, as a walker should be forced away from a gravitational hill. The effects of changing the line of sight parameter  $\sigma$  is similar to without a gravitational potential, as seen by the trails fusing into each other as  $\sigma$  is decreased.

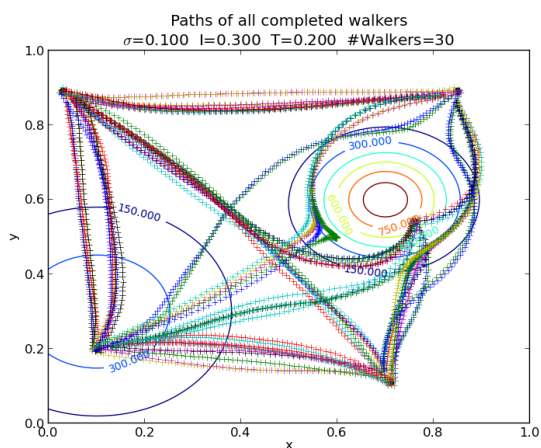




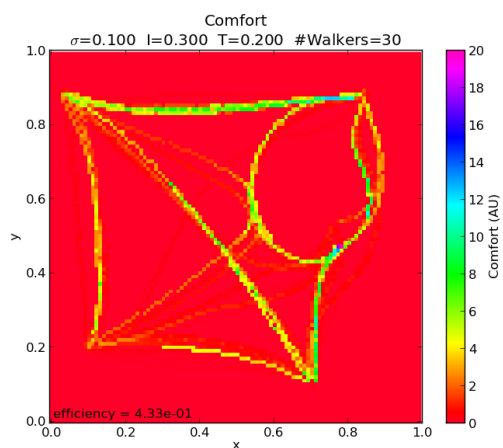
(a) Gaussian hill potential for  $\sigma = 0.5$ .



(b) Gaussian hill potential for  $\sigma = 0.5$ .

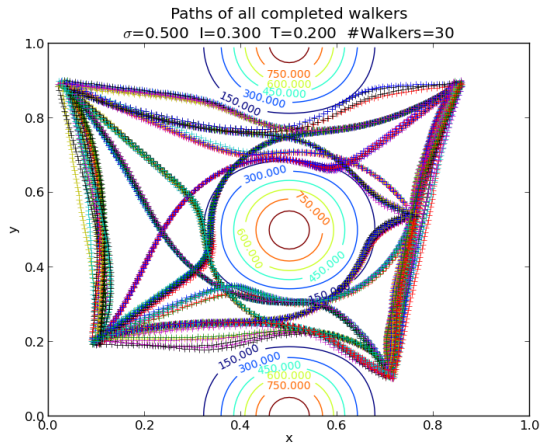


(c) Gaussian hill potential for  $\sigma = 0.1$ .

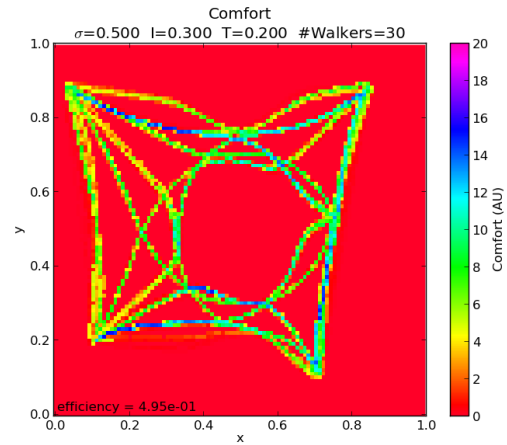


(d) Gaussian hill potential for  $\sigma = 0.1$ .

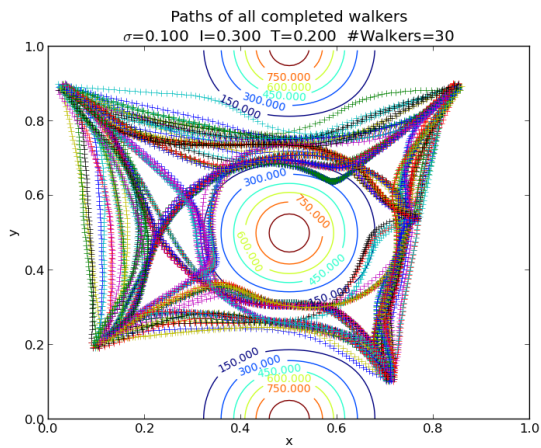
Figure 11: The Gaussian hill potential distorts the simplest path between the destinations. The walkers still manage to slightly increase the efficiency of the path network by clumping nearby paths together. Here,  $I = 0.3$ ,  $T = 0.2$ ,  $G_{max} = 20$ ,  $v_0 = 20$ ,  $N = 30$ , and  $\Delta = 0.0015$  for 2000 time steps.



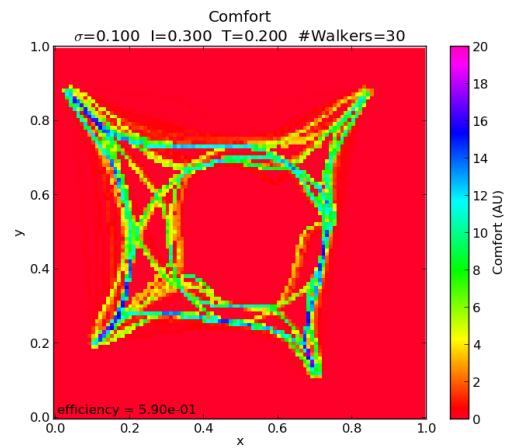
(a) Mountain range potential for  $\sigma = 0.5$ .



(b) Mountain range potential for  $\sigma = 0.5$ .

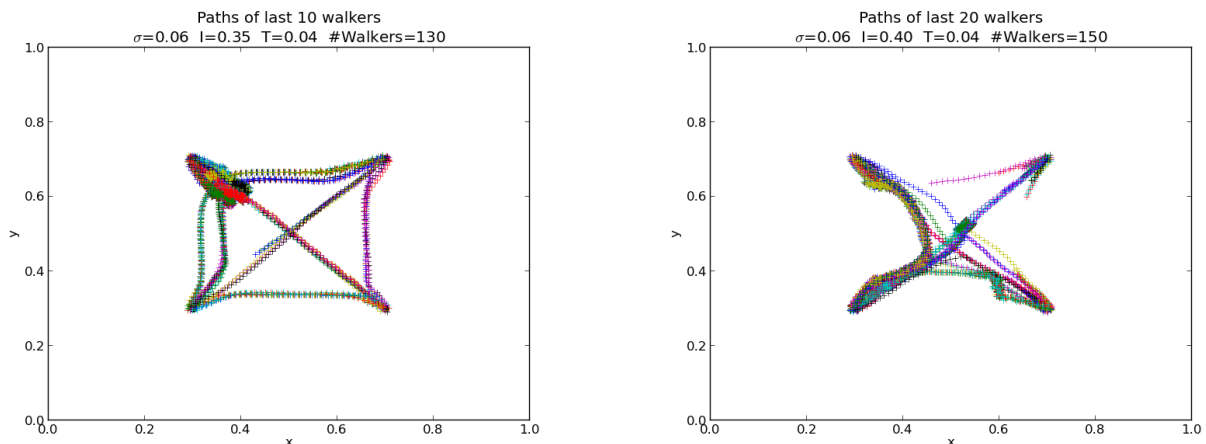


(c) Mountain range potential for  $\sigma = 0.1$ .



(d) Mountain range potential for  $\sigma = 0.1$ .

Figure 12: The mountain range potential distorts the simplest path between the destinations. The walkers still manage to optimize the network further. Here,  $I = 0.3$ ,  $T = 0.2$ ,  $G_{max} = 20$ ,  $v_0 = 20$ ,  $N = 30$ , and  $\Delta = 0.0015$  for 2000 time steps.



(a) Pooling of walkers near the north-west city.

(b) Pooling of walkers along the trails.

Figure 13: If the relative coupling to the paths is too strong compared to the coupling to the destination, then walkers will not finish their walks. This spurious effect can be removed by decreasing  $G_{max}$ , decreasing  $I$ , decreasing  $T$ , decreasing  $\sigma$ , increasing  $v_0$ , or decreasing the number of walkers. The values of these parameters for which pooling occurs are by no means universal and are sensitive to initial points of the walkers, the geometry of the cities, and the potential (if any is present).

## 6 Conclusion

We have demonstrated the emergence of trail networks using the Active Walker model. These trails were affected by various parameters, most notably  $\sigma$ , the visibility,  $I$ , the intensity of stepping, and  $T$ , the regeneration rate. We devised two metrics, the efficiency and the civility, to characterize the dynamics and the overall acceptability of a given set of trails to a system of active walkers. We found that low values of  $\sigma$  created high efficiency paths, while higher values created low efficiency, more direct pathways. In addition, changes in  $I$  and  $T$  affected both the efficiency and civility of the created paths. We have shown that this model can be an effective way to probe the formation of trail networks provided the values are chosen to prevent artifacts such as pooling.

## References

- [1] J. Deneubourg, S. Aron, S. Goss, and J.M. Pasteels, "The self-organizing exploratory pattern of the argentine ant," *Journal of Insect Behavior* **3** (2), 1990.
- [2] D. Helbing, P. Molnár, I. Farkas, K. Bolay, "Self-organizing pedestrian movement", *Environment and Planning B: Planning and Design*, **28** (361–383) 2001.
- [3] D. Helbing, J. Keltsch, P. Molnár, "Modelling the evolution of human trail systems," *Nature* **388** (47–50) 1997.
- [4] L. Verlet, "Computer 'experiments' on classical fluids. I. Thermodynamical properties of Lennard-Jones molecules," *Phys. Rev.*, **159** 1 (98–103) 1967.